

Temperature compensation for optical current sensors

W. Iain Madden
W. Craig Michie
Andrew Cruden
Pawel Niewczas
James R. McDonald

University of Strathclyde
Rolls Royce University Technology Centre
in Electrical Power Engineering
Department of Electrical Engineering
204 George Street
Glasgow G1 1XW
United Kingdom
E-mail: i.madden@strath.ac.uk

Ivan Andonovic
University of Strathclyde
Department of Electrical Engineering
Optoelectric Division
Glasgow, United Kingdom

1 Introduction

In the past 10 yr a great deal of research effort has been devoted to developing optical fiber sensors for measuring a wide range of physical and chemical parameters.¹⁻² Within the electricity industry, techniques for making voltage and current measurements have been of particular interest, principally for high voltage applications where substantial reductions in insulation requirements can be obtained.

Generally optical current transducers (OCTs) and voltage transducers (OVTs) are polarimetric devices. The voltage and current values to be measured are derived from the polarization rotation induced by either the electric field (in the case of an OVT) or the magnetic field (in an OCT) in the vicinity of a conductor. In most cases, exotic crystals or glasses³⁻¹² (e.g., TGG crystal or FR5 glass) are used as the active component that induces the polarization rotation. The sensitivity of these materials is strongly influenced by the operating temperature of the device, however, this is often overlooked. Here we evaluate the effect of temperature variations on the performance of an OCT. The analysis is supported by an experimental demonstration of an OCT over a range of operating temperatures and current values.

2 Optical Current Measurement

The OCT determines the current flow in an electrical conductor by measuring the magnetic field density within the vicinity of the conductor.³⁻¹² This change in polarization state is a function of the magnetic field strength, the interaction length and the Verdet constant of the material used to construct the device. Within the electricity industry, OCTs can be used for metering or protection purposes and must meet the related specification for that task. Two illustrative specifications are shown in Tables 1 and 2 and these are used as a benchmark within the following analysis.

Abstract. An analysis of an optical current transducer (OCT) considering in particular the influence of temperature induced variations in the Verdet constant is presented. The analysis is supported by an experimental evaluation of a prototype OCT over a range of operating temperatures and current values and concludes with a laboratory demonstration of a temperature compensation scheme that improves the measurement precision to better than 0.7%. © 1999 Society of Photo-Optical Instrumentation Engineers. [S0091-3286(99)01910-8]

Subject terms: magneto-optic transducer; Faraday effect; current measurement.

Paper 980152 received Apr. 17, 1998; revised manuscript received Dec. 17, 1998; accepted for publication Apr. 15, 1999.

The accuracy with which the current flow can be measured depends on the accuracy of the optical phase rotation measurement (the change in polarization state) and the confidence that can be placed in the model relating this information to the current flow.

The several sources of error in the polarization rotation measurement include electronic noise at the detector and intensity fluctuations. Vibration induced intensity fluctuations are considered elsewhere,⁵ here we are not concerned in detail with the physical origins of this error, only with the measurement precision that can be attained.

The effectiveness of the model is determined by the accuracy with which the Verdet constant of the optical sensor material is known and since this varies with temperature, the variation must be compensated to obtain the required measurement accuracy.

2.1 Temperature Sensitivity of the OCT

A host of different magneto-optic materials have been employed as the sensing medium in OCTs. These include high Verdet constant ferromagnetic and ferrimagnetic materials, such as yttrium iron garnet (YIG) and cadmium manganese telluride (CdMnTe), and low Verdet constant diamagnetic materials such as bismuth silicate (BSO) and even doped silica optical fiber itself. These different magnetic materials are classified according to their relative permeabilities (or susceptibilities), as shown in Table 3.

The amount of Faraday rotation θ (degrees) induced in the OCT is denoted by

$$\theta = VBl, \quad (1)$$

where V is the Verdet constant of the sensing medium,

Table 1 Specification of performance for a class 0.1 current transducer.

Percentage of rated operational current level	5	20	100	120
Specified measurement accuracy (%)	0.4	0.2	0.1	0.1

expressed in deg/T m, B is the magnetic flux density in Tesla and l is the interaction length (the length of the sensing material) measured in meters.

The Verdet constant is, however, a function of both wavelength and temperature.^{11,12} The former dependency is overcome by using a thermally stabilized light source; the latter is the focal point of this paper. From a review of Table 3 several points can be stated: the Verdet constant of materials are a function of their permeability, i.e., generally the higher the permeability the higher the Verdet constant; as the permeability increases the temperature dependency of the Verdet constant increases as well. For these reasons an appropriate compromise with regard to the selection of magneto-optic medium was a paramagnetic material which, for this paper, implies either TGG or Hoya FR-5 doped glass.

Two materials, TGG and FR5 glass, were selected for evaluation since both have relatively high Verdet constants and are widely available commercially. The Verdet constant of these materials was estimated from data supplied by the manufacturer and verified by experiment as^{5,11,12}

$$V_{FR5} = 1,853,370/T - 1708.36 \quad \text{deg/T m at } \lambda = 633 \text{ nm}$$

$$V_{FR5} = 429,242/T + 628.3 \quad \text{deg/T m at } \lambda = 850 \text{ nm} \quad (2)$$

$$V_{TGG} = 2,853,555/T - 2,833 \quad \text{deg/T m at } \lambda = 633 \text{ nm}$$

$$V_{TGG} = 1,346,463/T - 1,225 \quad \text{deg/T m at } \lambda = 850 \text{ nm}$$

Table 2 Specification of transducer performance for protection applications.

Percentage of rated operational current level	5	100	2,000	10,000
Specified measurement accuracy (%)	2	1	5	10

The variation of the preceding Verdet constants as described here is displayed in Fig. 1 at two optical wavelengths (633 and 850 nm) over a typical operational temperature range (250 to 350 K).

Since the measurement relies on the magnetic field producing a measurable polarization rotation, the material sensitivity is a central consideration in the design of an OCT. At any given temperature, TGG interrogated with a source wavelength of 633 nm has the highest Verdet constant and therefore it is reasonable to expect that this would be the optimum material choice. However, the variation in Verdet constant with temperature is also strongest in TGG at this operation wavelength and this may introduce errors that negate the benefits of using this particular crystal and wavelength combination. This is examined in more detail in the following sections.

2.2 Temperature Induced Error in Current Measurements

A large amount of work has been published on temperature compensation mechanisms for OCTs. Briefly, some of these mechanisms are as follows:

1. Direct variation of the polarization state of the light entering the sensor in such a manner as to oppose the thermal variation of the material Verdet constant. This was demonstrated using the natural temperature dependence of a wave plate, positioned before the sensing material.⁸
2. Interferometric phase measurements of temperature, combined with an intensity modulation measurement for the Faraday effect, have been used to simulta-

Table 3 Magnetic classification of materials.

Magnetic Class (example material)	Permanent Magnetic Moments?				Relative Permeability μ_r	Temperature Dependence of μ_r
	No	Yes				
		Parallel?	Antiparallel?	Unequal Order?		
Diamagnetic (bismuth silicate, BSO)	—	—	—	—	<1	Independent
Paramagnetic (terbium gallium garnet, TGG)	x	—	—	—	>1	$\propto \frac{1}{T}$
Ferromagnetic	—	x	—	—	$\gg 1$	Unique dependent on material (up to the Curie temperature)
Antiferromagnetic	—	—	x	—	$\gg 1$	Unique dependent on material (up to the Curie temperature)
Ferrimagnetic (yttrium iron garnet, YIG)	—	—	—	x	$\gg 1$	Unique dependent on material (up to the Curie temperature)

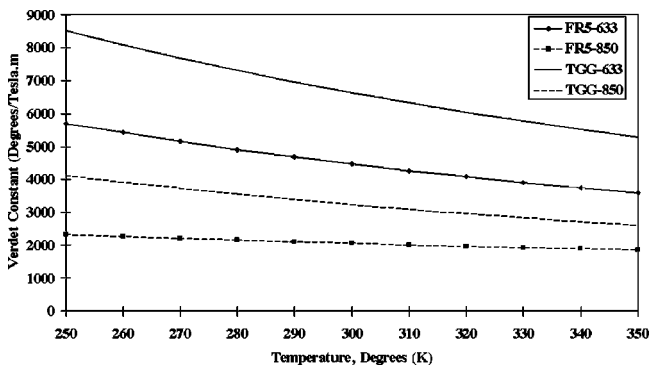


Fig. 1 Variation in Verdet constants of TGG and FR5 glass with temperature.

neously measure temperature and accurately compensate for its influence an OCT. This technique, where the temperature is measured over the same part of the sensing medium as the magneto-optic effect uses, enables precise compensation for temperature even in the presence of temperature gradients across the material.⁹

3. One method favored by many researchers to compensate for light intensity effects on the OCT, and employed by us, is to use a normalization algorithm given by

$$\text{Output} = \frac{I_{ac}}{I_{dc}},$$

where I_{ac} and I_{dc} are the ac and dc components of the original OCT output signal. This normalization has also been used, in a modified form, to provide a measure of temperature compensation given by

$$\text{Output} = \frac{I_{ac}}{1 + kI_{dc}},$$

where the term k can be introduced by appropriate orientation of the input polariser with respect to the Faraday medium crystal axis.^{6,10}

4. A more fundamental approach to providing temperature compensation is to use appropriate dopants during the crystal growth of YIG, to attempt to match the temperature dependencies of the Verdet constant and the material saturation magnetization, thereby providing “natural” compensation for thermal effects⁷ and an inherently stable material temperature characteristic.

All these techniques have their particular merits, however, we believe that the method demonstrated in this paper enables an appropriate compromise between the complexity of signal processing involved and the simplicity of sensor configuration and assembly.

2.3 Temperature Induced Error in Current Measurements

An initial assessment of the impact of temperature variation can be obtained by evaluating the difference between the Verdet constant at T_1 and the Verdet constant at $T_1 + \delta T$ (where δT represents a small error in temperature) for any given material and wavelength combination. This is shown

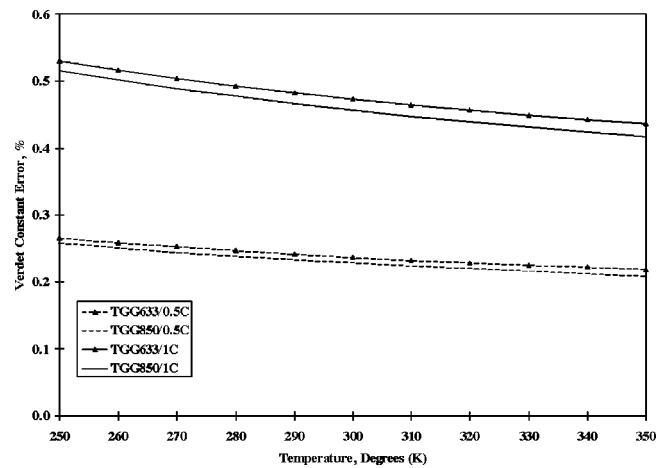


Fig. 2 Error in Verdet constant (TGG).

in Figs. 2 and 3 where, for illustration purposes, δT was set to 0.5 and 1°C. In all cases, it was assumed that the individual constants α and β are accurately known, i.e., no additional errors are introduced as a result of errors in these constants, although in practice this is unlikely to be the case since the coefficients are themselves derived from experiment and are therefore subject to experimental error.

Figures 2 and 3 reveal several interesting features. Assuming that there are no other sources of error, knowledge of the local temperature with 1°C accuracy enables the thermally induced variation in Verdet constant to be compensated for with sufficient accuracy to construct protection class instruments using any of the preceding materials. Class 0.1 metering devices, on the other hand, cannot be produced with any of these materials, even when the device operating temperature is known to better than 0.5°C. Over the entire range of operational temperatures, metering performance can be achieved only when sensor temperature is known to within 0.1°C (not shown).

The sensor with the best performance (i.e., it is least affected by temperature errors) is that constructed using FR5 glass and interrogated with an operational wavelength of 850 nm. Figure 1 shows that this FR5 glass has the

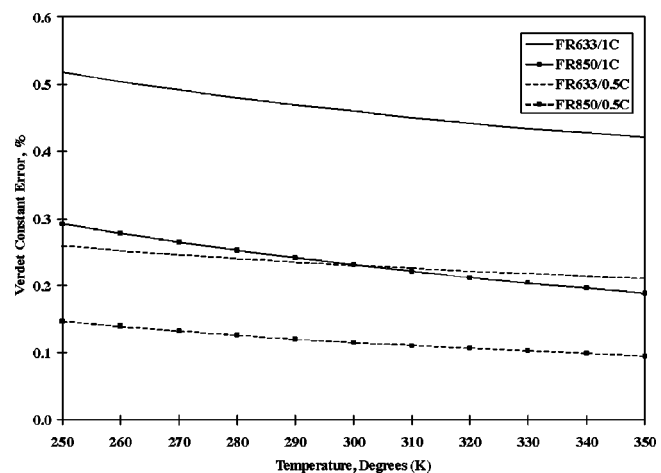


Fig. 3 Error in Verdet constant (FR5).

lowest Verdet constant of all of the material/wavelength combinations. It is therefore likely that it would have been rejected in favor of one of the other device combinations. The material and wavelength most likely to be selected from sensitivity considerations is TGG, using a source wavelength of 633 nm, which provides the poorest response to errors in the temperature measurement. TGG sensors require a temperature recovery precision of around 0.1°C (not shown) to achieve class 0.1 current metering specification.

2.3.1 Indirect recovery of sensor crystal temperature

The variation in Verdet constant with temperature is well known. Consequently several methods for determining the local temperature of the sensor have been investigated. Of these, the use of two independent interrogation wavelengths was considered to be potentially desirable since this method ensures that the exact crystal temperature will be recovered (to within the limits of the measurement process). The means for deriving the crystal temperature can be summarized as follows.

The optical rotation induced by the current within the conductor is measured at two operating wavelengths generating two related simultaneous equations:

$$\theta_1 = Bl(\alpha_1/T + \beta_1), \quad \theta_2 = Bl(\alpha_2/T + \beta_2). \quad (3)$$

The operating temperature can be recovered by first solving these equations, thus:

$$T = (\theta_1\alpha_2 - \theta_2\alpha_1) / (\theta_2\beta_1 - \theta_1\beta_2), \quad (4)$$

and this value is used to determine the magnetic field surrounding the conductor (and hence the current flowing through the conductor):

$$B_l = \theta_1 / \{[\alpha_1(\beta_1 - \beta_2\theta_1/\theta_2)] / [(-\alpha_1 + \alpha_2\theta_1/\theta_2) + \beta_1]\}. \quad (5)$$

The procedure is relatively simple to implement but successful operation requires accurate knowledge of the phase rotation angles θ_1 and θ_2 and the coefficients α and β (which must be determined experimentally). Errors in either of these can seriously degrade the measurement performance.

To illustrate the sensitivity of the measurement to phase recovery errors in particular, the accuracy of the temperature recovery procedure using the two wavelength interrogation scheme is illustrated in the following figures for examples where:

1. The current is assumed constant around a nominal working value (1000 A) and the temperature is cycled,
2. The temperature is maintained at 300 K and the current is cycled.

In both cases, it has been assumed that the polarization rotation can be recovered with a precision of up to 100 μ deg. This level of performance is broadly compatible with a metering class OCT (more details will be given

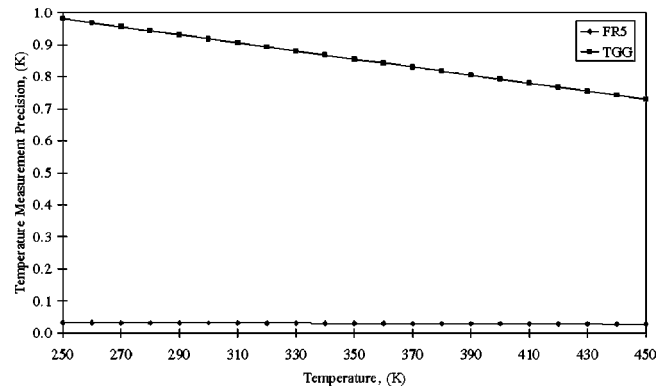


Fig. 4 Precision of temperature recovery process at full load current (1000 A) polarization rotation recovered with a precision 100 μ deg.

later) and therefore represents the operation of an optimized version of the presented system. The operation of an OCT rated at 1000 A is considered. The associated magnetic field at this current value has been calculated, for the bus bar geometry used to experimentally assess the sensor¹³ to be 4.04 mT. The magnetic field strength in a working environment is likely to be slightly higher than this but of the same order of magnitude, therefore the general trends that are obtained in the following analysis will be valid.

The results of these calculations are displayed graphically in Figs. 4 and 5. Clearly there is a significant difference between the operation of the TGG based sensor and the sensor made using FR5 glass. The rate of change in Verdet constant with temperature is insufficiently different in the case of the TGG sensor between the two wavelengths of 850 and 633 nm to enable the temperature to be accurately recovered. On the other hand, the FR5 based sensor recovers the temperature very accurately despite the fact that it has a significantly lower Verdet constant. Note that the TGG sensor performance was calculated assuming a device length of 2.5 cm as opposed to a device length of 10 cm for the FR5 sensor. This does significantly bias the calculation against the TGG device, however, the differences in device sizes reflects the practical differences in device construction (fuller details are given later). To complete the investigation, the operation of both sensors over the entire working range of current values must be esti-

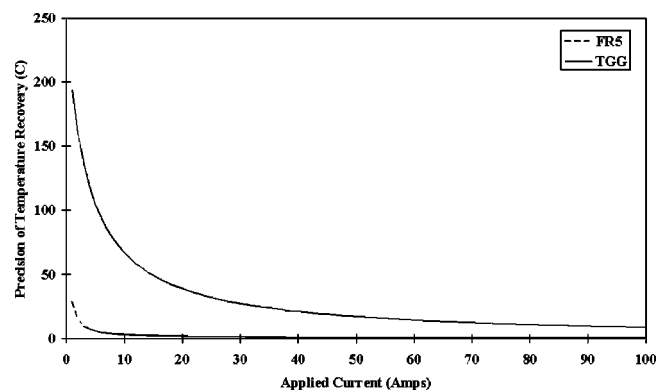


Fig. 5 Precision of temperature recovery process as a function of applied current.

Table 4 Performance specification of OCT, temperature error compensated to 0.1°C.

	TGG:633—2.5 cm	TGG:850—2.5 cm	FR5:633—10 cm	FR5:850—10 cm	TGG:543—2.5 cm
Approximate rotation at 1000 A	0.707 deg	0.345 deg	1.89 deg	0.85 deg	1.05 deg
Protection					
Precision of phase	625	350	1750	820	950
Recovery (μ deg)					
Metering					
Precision of phase	115	57	320	160	170
Recovery (μ deg)					

mated. At low current values, the errors in the phase recovery become increasingly more significant (as the polarization rotation is reduced) and hence the errors in the temperature recovery become more significant. Figure 5 shows the performance of both sensors over a range of currents from 1 to 100 A.

Earlier it was shown that to meet the specification for protection systems, the temperature of the sensor unit should be known to better than 1°C. The required accuracy for metering performance was significantly more stringent (0.1°C being required in the case of the TGG sensor). Clearly, none of the preceding sensor combinations have sufficient precision to meet this specification over the entire range of current values, the errors become increasingly more significant at low current values. The overall conclusion therefore is that a direct temperature measurement, using a method that is not influenced by the current flow within the conductor, is the most appropriate solution.

3 Current Measurement Characteristics

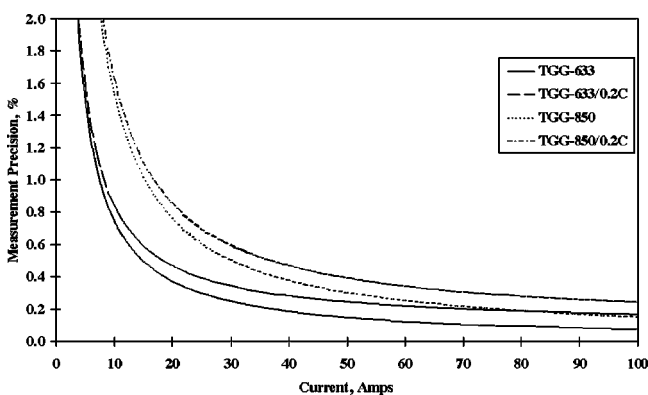
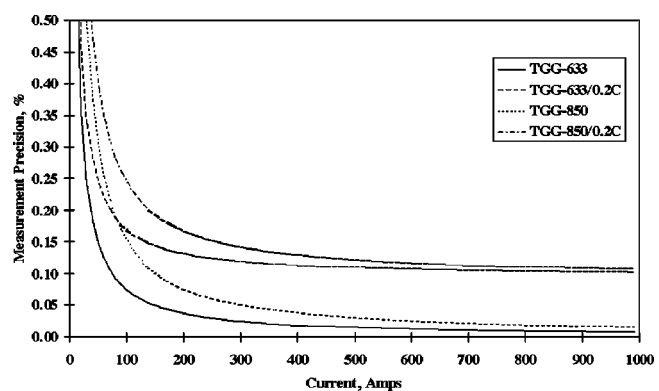
The specifications outlined in Table 1 describe operational requirements for OCT devices. As already demonstrated, temperature induced variations in the Verdet constant of the sensor material during the measurement process have a significant bearing on the overall performance. However, the primary consideration in the measurement process is the accuracy with which the induced polarization rotation can be recovered. To determine the relative significance of these two error contributions and to derive an OCT design a numerical evaluation of the OCT operation was performed using Matlab. Often the influence of two simultaneously varying parameters can be evaluated

analytically,^{14–19} however, in this case, the nonlinear variation of the Verdet constant with temperature prevents a solution from being readily derived. Several examples are provided to illustrate the application of the model to the problem and a detailed breakdown of the performance of a number of devices is summarized in Table 3 and Table 4 in Sec. 3.1.

In all of the following examples it is assumed that the polarization rotation can be recovered with a precision of 100 μ deg. The practicalities of achieving this performance are commented on in Sec. 4, note, however, that even with this level, the measurement errors are very significant at low currents. The predicted performance of a sensor made from a 5 cm length of TGG crystal is shown in Fig. 6.

The protection specification requires an accuracy of better than 2% at a current value of 5% of the nominal full load (i.e., in this case, 50 A). Clearly the precision of the preceding sensor is sufficient to meet this requirement. For metering applications the accuracy should be 0.4% at the 50 A current. Again all of the TGG characteristics are within this value, but only at the 633 nm interrogation wavelength. Additionally, for metering requirements, the OCT should be accurate to 0.2% at 20% of the full load current (200 A) and 0.1% at full load current. Figure 7 shows that compensating for temperature to 0.2°C is not sufficient to enable this goal to be reached.

Although it is possible to construct sensors with long (several centimeters) optical paths using samples of FR5 glass where a multiple pass geometry can be employed, this is not as readily achieved with TGG based sensors because the material itself is not widely available in adequately sized blanks. Even if it was possible to source the TGG in

**Fig. 6** Calculated OCT performance: TGG sensor, 5 cm.**Fig. 7** Calculated OCT performance: TGG sensor, 5 cm.

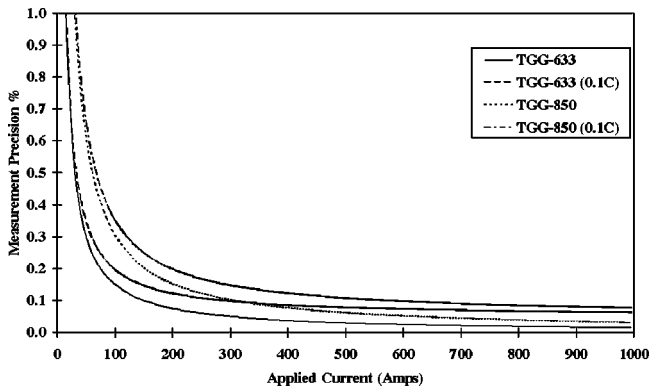


Fig. 8 Calculated OCT performance: TGG sensor, 2.5 cm.

this form, it is likely to be cost prohibitive. A realistic working length for the TGG sensor is therefore around 2.5 cm and this reduction in length degrades the overall performance. To meet the metering specification, the temperature compensation must be performed with the local temperature known to 0.1°C and then it can only be achieved with the operating wavelength of 633 nm, as shown in Fig. 8.

The same analysis was also carried out for the FR5 glass based sensor and is displayed in Figs. 9 and 10. In this case, however, the optical path length was set to 10 cm since this represents the path length of devices currently under test. The FR5 based sensor can be seen to meet the performance requirements for metering with a temperature measurement precision of 0.35°C . The surprising feature is, however, that the specification is only reached at the operational wavelength of 850 nm, where the Verdet constant is significantly lower.

3.1 Devices for Protection Applications

The performance of protection devices is considerably easier to meet than that of metering devices, enabling the precision in polarization recovery to be significantly relaxed. An analysis similar to that already carried out was repeated with the specific aim of determining the sensor specifications for protection applications. These findings, along with a summary of the sensor analysis for metering applications are summarized in Table 4. In addition to the wavelengths that are of present interest (633 and 850 nm)

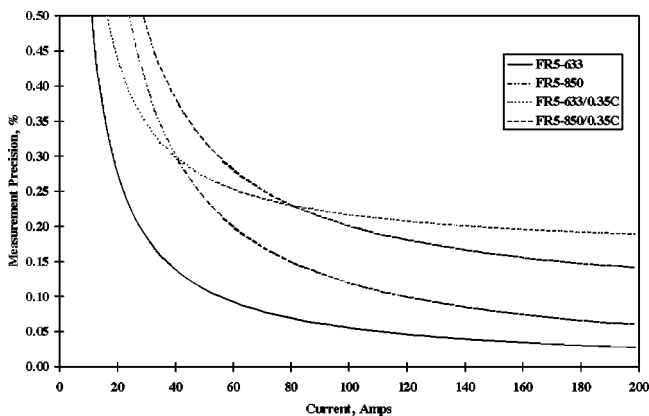


Fig. 9 Calculated OCT performance: FR5 sensor, 10 cm.

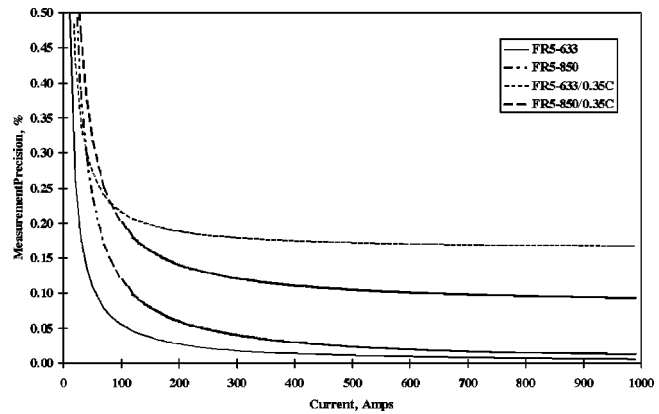


Fig. 10 Calculated OCT performance: FR5 sensor, 10 cm.

the operation of a device interrogated with a 543 nm source is also listed. Such devices are not readily obtainable at the moment but vertical cavity surface emitting laser (VCSEL) laser diodes with suitable output powers at low drive currents (several milliwatts at a 10 mA drive) are under development for display applications and these should be available in the near future.

Table 4 summarizes the precision with which the polarization rotation of the light traveling through the OCT must be recovered to construct devices with the required accuracy to meet protection and metering specifications. The main difference between the performances of the listed schemes lies simply in the fact that wavelength/material combinations that produce large phase shifts in response to the applied magnetic field require a lower phase measurement precision. Clearly for all cases, very precise measurements of optical polarization rotation are required to obtain the desired performances. These precision levels must be translated to accuracy performances in real devices. Thus all forms of potential offset and drift will have to be engineered out to better than the precision levels quoted earlier.

3.2 Detector Signal to Noise Performance

During the measurement process, the polarization rotation induced within the OCT crystal is converted to intensity by the analyzing polarizer and it is this intensity level that is measured to determine the current level. A key limiting factor will therefore be the electronic noise level present at the optical detector. The significance of the electronic noise level is described in the following analysis.

The output of the sensor is proportional to:

$$V_{\text{sensor}} \propto P_{\text{opt}} \cos^2(45 + \theta) + V_{\text{offset}}, \quad (6)$$

where θ is the optical phase rotation induced under the influence of the applied magnetic field, P_{opt} is the optical power at the receiver, and V_{offset} represents dc offsets that might arise through thermal drift in the electronic components or linear birefringence in the optics. This influence is ignored for the time being but must be addressed in the development of a fully operational sensor. The angular bias of 45 deg accounts for the orientation of the polarizers, thus the output of the detector is a voltage signal, which can be described as:

Table 5 OCT receiver noise performance specification. Temperature induced error is compensated to 0.1°C. The noise voltage represents the minimum resolvable voltage increment required to recover the rotation in polarization state.

	TGG:633—2.5 cm	TGG:850—2.5 cm	FR5:633—10 cm	FR5:850—10 cm	TGG:543—2.5 cm
V_{ac} at 1000 A	148 mV	72 mV	340 mV	178 mV	219 mV
Protection					
Receiver noise voltage	130 μ V	73 μ V	366 μ V	171 μ V	198 μ V
Metering					
Receiver noise voltage	24 μ V	12 μ V	67 μ V	33 μ V	36 μ V

$$V_{out} = (V/2)[1 - \sin(2\theta)], \quad (7)$$

i.e., there is a dc bias voltage of $V/2$ and an ac component of the signal (which contains the current information) described by $V \sin(2\theta)/2$. If the calculated levels of precision of required phase recovery for the measurement of the optical rotation are inserted into the preceding equation, then the required noise floor can be calculated for a specified bias voltage level.

The output of the present sensor is biased around a dc value of 6 V, i.e., the ac component of the signal is described by:

$$V_{ac} = 6 \sin(2\theta) V. \quad (8)$$

Hence the voltage swing at 1000 A and the required noise current can be calculated for each sensor. These are listed in Table 5. The rotation of polarization state has been calculated assuming a 2.5 cm length of crystal for the TGG sensor and a 10 cm active sensor length for the FR5 sensor operating at 290 K.

Examining Tables 4 and 5 gives a clear illustration of the scale of the measurement problem. In essence, the small phase rotations that are observed at low current values restrict the operation of the device to the extent that a very high SNR must be achieved at the receiver to meet the specification for metering or protection. To alleviate some of this burden on the detector electronics, the optical rotation over the operational range can be increased. This means that either sensors with longer interaction lengths, or materials with higher Verdet constants are required.

At the moment, the most promising candidate for a protection device of those examined earlier in the paper is that manufactured from FR5 glass, with a 10 cm optical path length, temperature compensated to 0.1°C and interrogated with a source wavelength of 633 nm. In this instance, sensors with sufficient precision to produce practical devices can be realized with receiver noise levels in the region of 500 μ V. The increase in Verdet constant, that can be obtained by shifting the wavelength of operation to shorter wavelengths, e.g., around 540 nm where LED and VCSEL sources are becoming available will improve the performance of the TGG sensor to a level comparable to that of the FR5 sensor. Although the sensitivity of TGG to temperature drifts is higher at this wavelength, compensating the sensor to account for temperature changes of around 0.1°C will be sufficient to meet the operational requirements.

Note that the preceding calculations assume that the all noise sources, including vibration effects, are reduced to the below levels quoted earlier. In practice, this may be difficult to achieve. To implement the vibration compensation scheme, however, two counter propagating light sources are used.⁵ This has the net effect of doubling the optical interaction length and this will, in turn, relax the operational specification of the sensor.

In the preceding illustration, the departure from a linear model at high operational currents was ignored. This will have the most significant impact on protection devices where the device may be driven outside the sinusoidal range of its characteristics. This represents an additional complication that can be resolved with appropriate processing but that does add to the complexity of the demodulation system. However, the alternative of placing greater demands on the detector electronics is extremely difficult, as already illustrated. Note also that the preceding analysis has assumed that a noise floor, in millivolts, takes into account all sources of noise—including vibration effects.

3.3 Comparison with Experimental Data

To assess the general validity of the preceding analysis the results were compared with an experimental investigation carried out within the laboratory. Two variations of the OCT are currently undergoing development, an FR5 based sensor (which enables a total optical path length of 10 cm to be obtained using a multipass geometrical arrangement) and TGG based sensor (with a total optical path length of 1.5 cm). The TGG sensor is presently being used to evaluate the performance of a temperature compensation scheme using a thermocouple to determine the TGG crystal temperature. The results from this experiment, as the applied current level was cycled from 1 to 1000 A, were used to gauge the performance of the model.

The precision of the phase recovery was estimated from the receiver SNR, which at an applied current level of 1000 A was determined to be around 200. Since the optical rotation at this level is estimated to be around 0.2 deg, the measurement precision was estimated to be approximately one hundredth of this value, around 0.001 deg. Figure 11 shows that over the measurement range, the model and experiment are in good agreement.

4 Experimental Evaluation of OCT Temperature Compensation Scheme

The analysis presented in Sec. 3 demonstrated that precise temperature compensation is required to enable effective

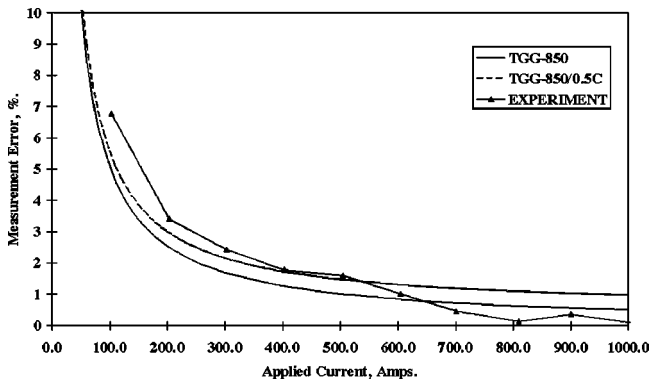


Fig. 11 Experimental current measurement using TGG sensor.

operation of OCT devices. Additionally it was reported that indirect recovery of temperature by interrogating the device at two separate wavelengths was not likely to be effective at low current levels. Therefore it was concluded that a means of directly measuring the temperature used to compensate the sensor output was required. The operating principle was proved in the first instance using a thermocouple to provide the temperature information.

To obtain accurate and reliable measurements of the TGG crystal temperature, a thermocouple was mounted within the sensor housing in close proximity to the sensing material. Figure 12 schematically illustrates the electronic section of the temperature compensation scheme implemented. The output of the thermocouple was amplified and fed into an analogue to digital convertor (ADC), the output of which was then used as an input address for an electrically programmable read-only memory (EPROM) look-up table containing the compensation characteristics for the optical material used. The digital to analogue convertor (DAC) generates the required conversion signal, which is multiplied with the OCT output signal to produce a compensated output.

4.1 Experimental Evaluation

Figure 13 shows the arrangement used to control the temperature of the current sensor unit. The TGG current sensor was located within a polytetrafluoroethylene (PTFE) box and an aluminum heat sink placed over the sensor to assist with the heat transfer mechanism. Two Peltier thermoelectric elements were placed between the heat sink and an upper tray containing coolant during the temperature cycling tests. The use of the coolant (a combination of dry ice

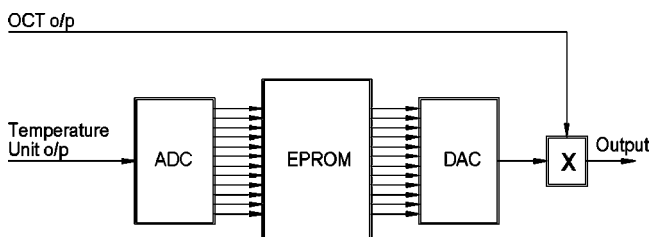


Fig. 12 Functional specification of the direct measure temperature compensation scheme.

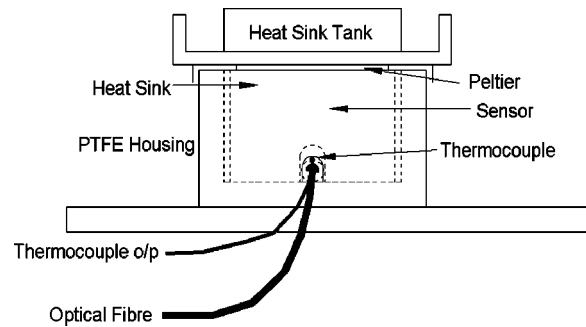


Fig. 13 Experimental arrangement for temperature control of the sensor environment.

and methylated spirit) enabled stable temperature conditions to be achieved at temperatures down to -20°C .

The output of the OCT was measured at a constant current level of 1000 A while the temperature was cycled from -20 to 100°C . The variation in the output signal from the OCT transducer was then used to construct the temperature compensation look-up curve to be stored within the EPROM. Temperature cycles were then repeated and the look-up table used to correct the OCT output for temperature fluctuations. Figure 14 shows the actual sensor output along with the compensated signal. The change in sensor output over the tested temperature range has been reduced from $\pm 18\%$, uncompensated, to $\pm 0.7\%$ with compensation.

5 Conclusions

This paper has described in detail the performance of an OCT considering the influence of electronic noise of the measurement performance. It was shown that temperature compensation to within 1°C is, in principle, sufficient for protection class devices to be realized, however, practical sensors are likely to require a greater degree of temperature compensation. To operate a metering class device effectively, the temperature of the sensor must be known to within 0.1°C . The analysis is supported by an experimental evaluation that shows good agreement with the theoretical predictions.

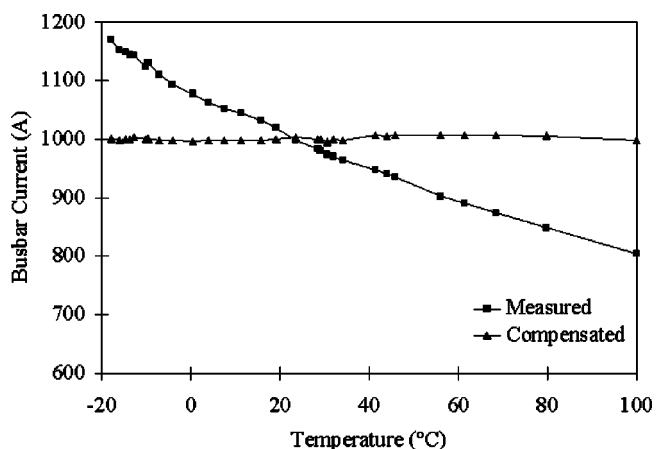


Fig. 14 Comparison between the direct and compensated sensor outputs.

A temperature compensation scheme based on a direct temperature measurement and a digital look-up table was constructed and evaluated in the laboratory. This method was shown to reduce temperature induced errors from 20 to less than 1%. Further improvements are anticipated as the engineering of the system is refined.

Acknowledgments

The authors wish to acknowledge the support of Rolls Royce Transmission and Distribution for support for this work and in particular Mr. A. Bennett, B. Taylor and P. Ozers for technical guidance.

References

1. E. Udd, *Fibre Optic Sensors: An Introduction for Engineers and Scientists*, Wiley and Sons, New York (1991).
2. J. Dakin and B. Culshaw, *Optical Fibre Sensors: Applications IV*, Artech House, Boston (1997).
3. A. Cruden, Z. J. Richardson, J. R. McDonald, and I. Andonovic, "Optical-crystal based devices for current and voltage measurement," *IEEE Trans. Power Deliv.* **10**(3), 1217–1223 (1995).
4. A. Cruden, Z. J. Richardson, J. R. McDonald, I. Andonovic, W. Laycock, and A. Bennett, "Compact 132kV combined optical voltage and current measurement system," in *Proc. IEEE Instrumentation & Measurement Technology Conf.*, Chap. 294, 1399–1402 (1997).
5. P. Niewczas, A. Cruden, C. Michie, I. Madden, and J. McDonald, "Vibration compensation technique for an optical transducer," *Opt. Eng.* (in this issue).
6. P. Menke and T. Bosselmann, "Temperature compensation in magneto-optic AC current sensors using an intelligent AC-DC signal evaluation," *J. Lightwave Technol.* **13**(7), 1362–1370 (1995).
7. M. N. Deeter, A. H. Rose, and G. W. Day, "Fast, sensitive magnetic field sensors based on the Faraday effect in YIG," *J. Lightwave Technol.* **8**(12), 838–842 (1990).
8. P. A. Williams, G. W. Day, and A. H. Rose, "Compensation for Temperature dependence of Faraday effect in diamagnetic materials: application to optical fibre sensors," *Electron. Lett.* **27**(13), 1131–1132 (1991).
9. S. H. Zaidi and R. P. Tatam, "Faraday-effect magnetometry: compensation for the temperature dependent Verdet constant," *J. Meas. Sci. Technol.* **5**, 1471–1479 (1994).
10. E. A. Ulmer, "A high-accuracy optical current transducer for electric power systems," *IEEE Trans. Power Deliv.* **5**(2), 892–898 (1990).
11. HOYA Corporation, USA, FR5 Data Sheet (1995).
12. N. P. Barnes and L. B. Petway, "Variation of the Verdet constant with temperature of terbium gallium garnet," *J. Opt. Soc. Am. B* **9**(10), 1912–1915 (1992).
13. P. Niewczas, "Comparative testing of electro-magnetic field modelling software: evaluation of the magnetic field behaviour along a longitudinal section of magneto-optic crystal," Report RR/OPT/TR/1996-004, internal report, Univ. of Strathclyde (1996).
14. F. Farahi, D. J. Webb, D. C. Jones, and D. A. Jackson, "Simultaneous measurement of temperature and strain: cross-sensitivity consideration," *J. Lightwave Technol.* **8**(2), 138–142 (1990).
15. A. M. Vengsarkar, W. C. Michie, L. Jankovic, B. Culshaw, and R. O. Claus, "Fiber-optic dual-technique sensor for simultaneous measurement of strain and temperature," *J. Lightwave Technol.* **12**(1), 170–177 (1994).
16. V. Gusmeroli and M. Martinelli, "Non-incremental interferometric fiber-optic measurement method for simultaneous detection of temperature and strain," *Opt. Lett.* **19**(24), 2164–2166 (1994).
17. M. G. Xu, J.-L. Archambault, L. Reekie, and J. P. Dakin, "Simultaneous measurement of strain and temperature using fibre grating sensors," in *10th Int. Conf. on Optical Fibre Sensors*, B. Culshaw and J. D. C. Jones, Eds., *Proc. SPIE* **2360**, 191–194 (1994).
18. W. Jin, W. C. Michie, G. Thursby, M. Konstantaki, and B. Culshaw, "Geometric representation of simultaneous measurement of temperature," *Opt. Eng.* **36**(8), 2272–2278 (1997).
19. W. Jin, W. C. Michie, G. Thursby, M. Konstantaki, and B. Culshaw, "Simultaneous measurement of temperature and strain: error analysis," *Opt. Eng.* **36**(2), 598–609 (1997).

Biographies of the authors appear with the paper "Vibration compensation technique for an optical transducer" in this issue.